Table S1. List of fatty acids assayed in this study. Peak emission (λ_{max}) presented as mean ± SEM (n=3).

Name	Class	C atom #	DB #	ω-pos	Nile Blue λ_{max} 660 nm	Nile Red λ_{max} 575 nm
Cholesterol	Cholesterol	27	1	-	171 ± 4	597 ± 15
Cholesteryl linoleate	Cholesterol ester	45	2	-	281 ± 5	989 ± 22
Cholesteryl oleate	Cholesterol ester	45	3	-	197 ± 8	1230 ± 20
1-oleoyl-2-sn-2-glycerol	Diglyceride	37	0	-	154 ± 10	781 ± 16
Galactoceramide	Phospholipid	40	1	-	130 ± 4	200 ± 14
Glucosylceramide	Phospholipid	46	1	-	603 ± 30	2574 ± 150
L-a-phosphatidyl choline	Phospholipid	42	2	-	437 ± 15	1086 ± 40
Platelet activating factor (PAF)	Phospholipid	26	0	-	451 ± 50	1244 ± 53
Phosphatidyl ethanolamine	Phospholipid	41	2	-	315 ± 14	155 ± 6
Phosphatidyl serine	Phospholipid	42	2	-	480 ± 30	647 ± 26
Phosphatidylinositol (3,4,5)-triphosphate	Phospholipid	47	4	-	130 ± 9	40 ± 2
Sphingomyelin	Phospholipid	47	2	-	160 ± 6	322 ± 22
Myelin basic protein	Protein	-	-	-	134 ± 8	248 ± 5
High density lipoprotein	Protein	-	-	-	1038 ± 44	1289 ± 50
Low density lipoprotein	Protein	-	-	-	661 ± 26	2076 ± 70
Propionic Acid	Saturated	3	0	-	47 ± 3	96 ± 5
Glycerol	Saturated	3	0	-	111 ± 5	120 ± 12
O-phosphorylethanolamine	Saturated	3	0	-	100 ± 5	100 ± 8
Butyric acid	Saturated	4	0	-	282 ± 10	35 ± 2
Hexanoic acid	Saturated	6	0	-	127 ± 8	55 ± 6
D-galactose	Saturated	6	0	-	130 ± 12	135 ± 20
Decanoic acid	Saturated	10	0	-	52 ± 2	119 ± 24
Lauric Acid	Saturated	12	0	-	20 ± 1	10 ± 1
Myristic acid	Saturated	14	0	-	18 ± 2	110 ± 14
Pentadecanoic acid	Saturated	15	0	-	144 ± 6	154 ± 19
Palmitic acid	Saturated	16	0	-	92 ± 4	276 ± 25
Stearic acid	Saturated	17	0	-	107 ± 4	103 ± 10
Heptadecanoic acid	Saturated	17	0	-	361 ± 15	122 ± 10
Nonadecanoic acid	Saturated	19	0	-	37 ± 2	65 ± 4
Arachidic acid	Saturated	20	0	-	414 ± 15	53 ± 4
Heneicosanoic acid	Saturated	21	0	-	91 ± 6	37 ± 5
Lignoceric acid	Saturated	24	0	-	53 ± 4	18 ± 4
Octanoic acid	Saturated	8	0	-	14 ± 1	72 ± 10
Triacetate	Saturated - triglyceride	9	0	-	88 ± 10	120 ± 11
Tributyrate	Saturated - triglyceride	15	0	-	120 ± 15	164 ± 14

Trihexanoate	Saturated - triglyceride	21	0	-	73 ± 9	1186 ± 91
Tridecanoate	Saturated - triglyceride	33	0	-	138 ± 12	3065 ± 180
Tridodecanoate	Saturated - triglyceride	39	0	-	82 ± 8	319 ± 29
Tripalmitate	Saturated - triglyceride	51	0	-	41 ± 3	540 ± 33
Tripalmitoleate	Saturated - triglyceride	51	3	7	203 ± 17	3515 ± 220
Trioleate	Saturated - triglyceride	57	3	9	175 ± 19	2121 ± 159
Trilinoleate	Saturated - triglyceride	57	6	9	70 ± 5	1412 ± 144
Oestrogen	Steroid	18	3	-	66 ± 4	53 ± 3
Estrone	Steroid	18	3	-	31 ± 3	147 ± 6
Dihydrotestosterone	Steroid	19	0	-	161 ± 6	282 ± 10
Testosterone	Steroid	19	0	-	102 ± 4	137 ± 8
Corticosterone	Steroid	21	1	-	154 ± 5	32 ± 2
Deoxycorticosterone	Steroid	21	1	-	120 ± 5	149 ± 9
Progesterone	Steroid	21	1	-	76 ± 2	147 ± 8
Crotonic acid	Unsaturated	4	1	2	111 ± 9	21 ± 1
7-Octenoic acid	Unsaturated	8	1	5	136 ± 5	37 ± 1
2-Decenoic acid	Unsaturated	10	1	5	90 ± 10	50 ± 2
5-Dodecanoic acid	Unsaturated	12	1	7	71 ± 5	117 ± 10
Myristoleic acid	Unsaturated	14	1	5	36 ± 2	37 ± 2
Palmitoleic acid	Unsaturated	16	1	7	1585 ± 41	193 ± 5
Linoleic acid	Unsaturated	18	2	6	1713 ± 67	142 ± 9
Oleic acid	Unsaturated	18	1	9	1867 ± 59	600 ± 30
a-linolenic acid	Unsaturated	18	3	6	244 ± 22	217 ± 15
Cis-vaccenic acid	Unsaturated	18	1	7	1455 ± 35	361 ± 19
Arachadonic acid	Unsaturated	20	4	6	1338 ± 29	348 ± 22
Eicosenoic acid	Unsaturated	20	1	9	1057 ± 49	210 ± 11
Eicosapentanoic acid	Unsaturated	20	5	3	663 ± 25	244 ± 14
1-monooleoyl-rac-glycerol	Unsaturated	21	1	9	130 ± 8	30 ± 2
Erucic acid	Unsaturated	22	1	9	1650 ± 85	335 ± 10
Decosahexanoic acid	Unsaturated	22	6	3	418 ± 45	234 ± 11
Anandamide	Unsaturated	22	4	6	178 ± 24	525 ± 45
Nervonic acid	Unsaturated	24	1	9	894 ± 37	298 ± 29
Palmitelaidic acid	Unsaturated - trans	16	1	7	228 ± 11	109 ± 4
Elaidic acid	Unsaturated - trans	18	1	9	779 ± 38	187 ± 14
Linoelaidic acid	Unsaturated - trans	18	2	6	529 ± 15	62 ± 9
Trans-vaccenic acid	Unsaturated - trans	18	1	7	716 ± 18	303 ± 16
11(E)-Eicosenoic acid	Unsaturated - trans	20	1	9	360 ± 11	91 ± 10
Mineral oil		-	-	-	5 ± 1	1237 ± 122

Table S2. ***Pairwise comparisons of changes in Nile Red fluorescence in the yolk sac across development. P values given, NS = non significant difference.***

Embryonic day (E)	10.5	11.5	12.5	13.5	14.5	15.5	16.5	17.5	18.5
10.5		*NS*	*NS*	*NS*	*<0.0001*	*<0.0001*	*<0.0001*	*<0.0001*	*<0.0001*
11.5			*NS*	*NS*	*<0.0001*	*<0.0001*	*<0.0001*	*<0.0001*	*<0.0001*
12.5				*NS*	*<0.0001*	*<0.0001*	*<0.0001*	*<0.0001*	*<0.0001*
13.5					*<0.0001*	*<0.0001*	*<0.0001*	*<0.0001*	*<0.0001*
14.5						*NS*	*NS*	*NS*	*NS*
15.5							*NS*	*NS*	*NS*
16.5								*NS*	*NS*
17.5									*NS*
18.5									

Table S3. ***Pairwise comparisons of changes in Nile Blue fluorescence in the yolk sac across development. P values given, NS = non significant difference.***

Embryonic day (E)	10.5	11.5	12.5	13.5	14.5	15.5	16.5	17.5	18.5
10.5		*NS*	*NS*	*0.0195*	*<0.0001*	*<0.0001*	*0.0012*	*<0.0001*	*NS*
11.5			*NS*	*0.0261*	*<0.0001*	*<0.0001*	*0.0018*	*<0.0001*	*NS*
12.5				*NS*	*0.0111*	*0.0008*	*NS*	*NS*	*NS*
13.5					*NS*	*0.0357*	*NS*	*NS*	*NS*
14.5						*NS*	*NS*	*NS*	*0.0245*
15.5							*NS*	*NS*	*0.0016*
16.5								*NS*	*NS*
17.5									*NS*
18.5									

Table S4. Principal component analysis correlation matrix for data presented in adult mouse liver SPADE analysis. Significance (1-tailed): * $p<0.05$; ** $p<0.01$

	FSC	SSC	CD11b	NR	PI	EpCAM	NB	F4/80	VitA
Size		*0.546***	*0.247***	*0.061*	*-0.017*	*0.120**	*0.276***	*0.005*	*0.317***
Granularity			*0.356***	*0.635**	*0.287***	*0.240***	*0.641***	*0.137**	*0.844***
CD11b				*0.117**	*-0.422***	*0.232***	*0.520***	*0.204***	*0.560***
NR					*0.501***	*0.349***	*0.501***	*0.301***	*0.747***
PI						*0.202***	*0.231***	*-0.013*	*0.255***
EpCAM							*0.367***	*0.614***	*0.366***
NB								*-0.006*	*0.801***
F4/80									*0.210***
VitA									

Table S5. Fluorescently-conjugated antibodies used for multiparametric flow cytometric analyses in the mouse liver.

Antibody	Fluorophore	Cat #	Clone	Source	Citation
Anti-mouse F4/80	APC	123115	BM8	BioLegend	Schaller, E *et al*. *Mol. Cell. Biol.* 22:8035. (2002)
Anti-mouse CD326 (EpCAM)	PerCP/Cyanine 5.5	118219	G8.8/	BioLegend	Dooley, J *et al*. *J Immunol.* 175:4331. (2005).
Anti-mouse/human CD11b	FITC	101205	M1/70	BioLegend	Iwasaki, A and Kelsall, B. L. 2001. *J. Immunol.* 166:4884 (2001).

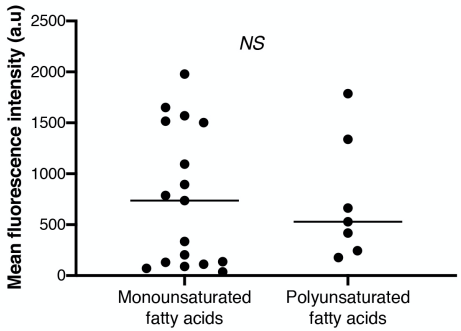

Figure S1: No differences in Nile Blue fluorescence between mono- and polyunsaturated fatty acids.
Spectrofluorimetric analyses of unsaturated fatty acids in the presence of Nile Blue comparing mono- and polyunsaturated fatty acids. Fatty acids were reconstituted in DMSO and pipetted onto a 96-well plate at a final concentration of 100 µmol.L^{-1}. Nile Blue was added to a final concentration of 1 µmol.L^{-1} and excited at 620 nm. Emission was collected from 640 to 800 nm. Data presented as mean ± SEM (n=3). Significant differences between monounsaturated and polyunsaturated fatty acids were determined by Students *t*-test.

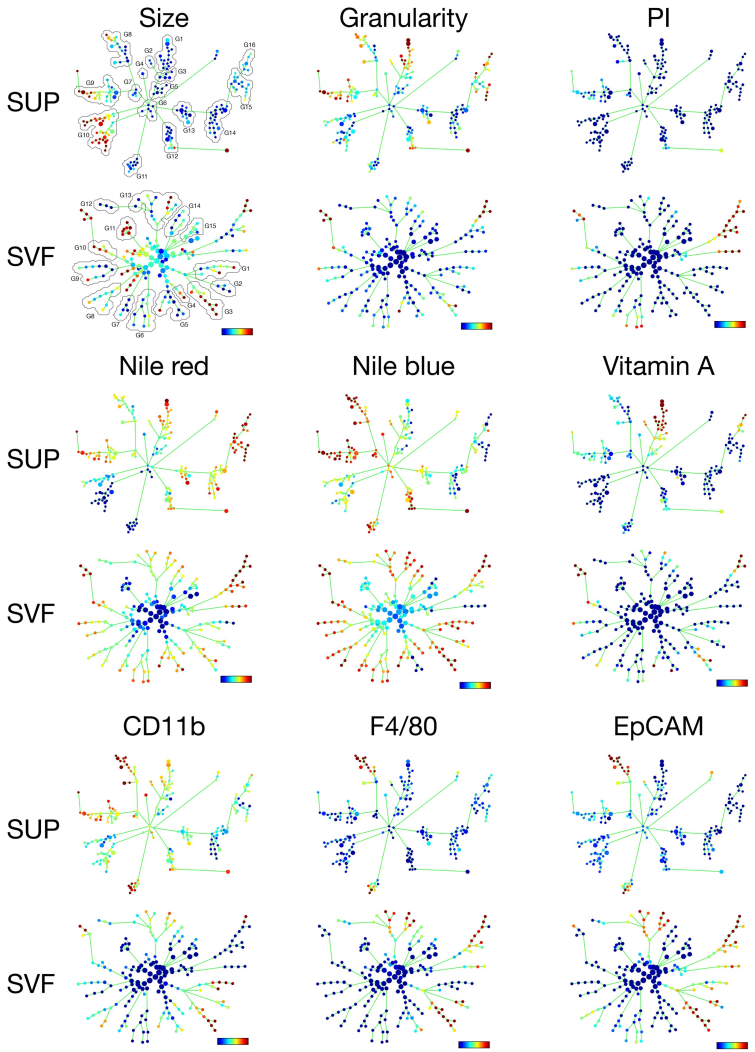

Figure S2: Multiparametric, flow cytometric analyses of hepatic tissue organised by SPADE plots distinguish clusters of lipid rich populations.
Spanning-tree Progression Analysis of Density-Normalised Events' (SPADE)[40] analyses were conducted on the buoyant fraction (BF) and stromal vascular fraction (SVF) of dissociated mouse livers stained with Nile Red, Nile Blue, F4/80, EpCAM, CD11b and propidium iodide. Side scatter (granularity), forward scatter (size) and propidium iodide (PI) were also used to build the SPADE tree consisting of a total of 200 nodes. Each node represents a cluster of cells. Blue coloured nodes indicate low levels of fluorescence for the respective marker while red indicates high levels of fluorescence. Clusters of nodes were grouped together according to differences in fluorescence intensity.

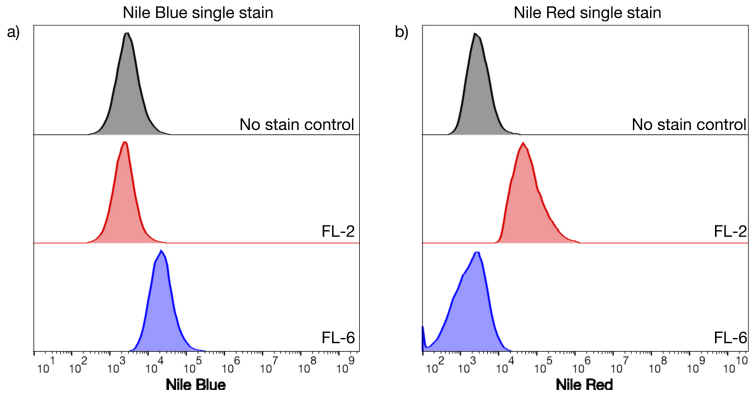

Figure S3: Nile Blue and Nile Red do not overlap in spectral emission by flow cytometry. Single cell suspensions of white adipose tissue were generated using the method previously published[16]. Cells of the buoyant fraction were stained with either Nile Blue (a) or Nile Red (b) and fluorescent populations identified. Fluorescent channel (FL) 6 is excited by the 620 nm laser and detects emission at 660 ± 20 nm. Fluorescent channel (FL) 2 is excited by the 488 nm laser and detects emission at 575 ± 30 nm. Nile Blue (blue shaded plot) and Nile Red (red shaded plot) are only detected in the FL-6 and FL-2 respectively. The black shaded plot represents the no-stain control.

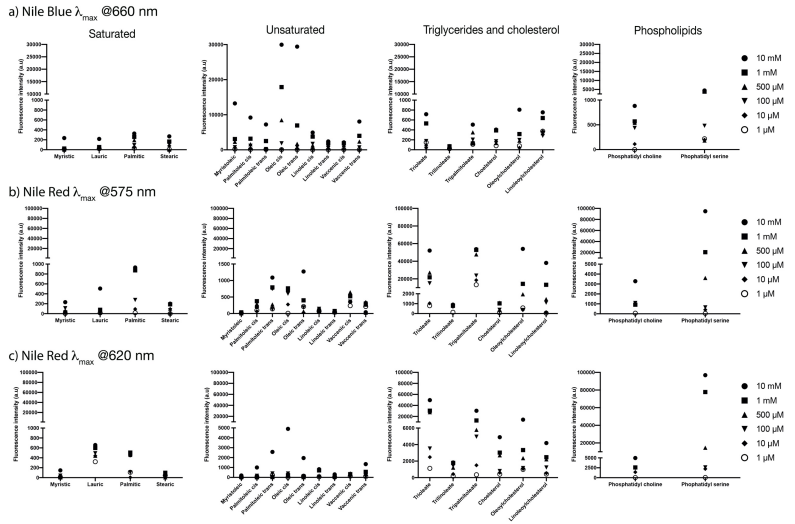

Figure S4: Increasing lipid concentration elicits greater Nile Blue and Nile Red fluorescence.
Spectrofluorimetric analyses of lipids from multiple classes (saturated and unsaturated free fatty acids, cholesterol, cholesterol esters, triglycerides and phospholipids) were performed in the presence of Nile Blue and Nile Red. A dose-response was performed to determine the relationship between lipid concentration and Nile Blue and Nile Red fluorescence. The concentration of lipids ranged from 1 µM - 10 mM. Nile Blue was excited at 620 nm while Nile Red was excited at 488 nm. Peak emission (λ_{max}) for Nile Blue (a) was collected at 660 nm; at 575 nm (b) and 620 nm (c) for Nile Red.